CNS CaThe Validation

Cambridge Numerical Solutions Ltd

November 2024

This report presents an experimental validation of CaThe, the CNS thermochemical software for energetic materials. The adopted approach involves using CaThe to calculate the detonation velocity (VOD) for a broad range of energetic materials, followed by a comparison with corresponding experimental data from the literature. The report evaluates the model's accuracy using various statistical measures to assess VOD errors, and confirms that CaThe can reliably capture correct detonation velocities for explosives of varying compositions and initial densities. Additionally, the report validates the module's capability to model isentropic expansions, with calculated isentropes compared to experimentally calibrated Jones-Wilkins-Lee (JWL) reference curves, highlighting CaThe's potential for generating equation of state (EOS) data for use in direct numerical simulations of explosives.

1 VOD calculation

To conduct this validation exercise, we consider a large dataset of explosives with diverse properties. For each entry, we perform a calculation in CaThe to determine its detonation properties. This section compares the calculated and corresponding experimental detonation velocities across the explosives included in the study.

The dataset, originally compiled by Hobbs and Baer [1], spans explosives of various compositions and initial densities, providing a robust test for assessing CaThe's predictive accuracy. Detailed information for each explosive, including experimental and calculated detonation velocities, can be found in Table 3 (Appendix A).

Figure 1 graphically illustrates this same data as a scatter plot comparing experimental ($x-$axis) and calculated ($y-$axis) detonation velocities for all explosives. Each point represents a single explosive, and the proximity of the points to the $x = y$ line indicates the level of agreement between the model's predictions and experimental measurements. The clustering of points around this line, with the majority falling well within the $\pm 5\%$ shaded bands, demonstrates a strong correlation and highlights the model's reliability across a wide range of explosives.

To quantitatively assess CaThe's performance, we calculate the root mean squared error (RMSE), mean absolute error (MAE) and maximum absolute error (MaxAE) between the experimental and calculated VODs. These metrics are defined as follows:

$$\mathrm{RMSE} = \sqrt{\frac{1}{N}\sum_{i=1}^{N}\left(\frac{\mathrm{VOD}_i^{exp} - \mathrm{VOD}_i^{calc}}{\mathrm{VOD}_i^{exp}}\right)^2}, \tag{1}$$

$$\mathrm{MAE} = \frac{1}{N}\sum_{i=1}^{N}\left|\frac{\mathrm{VOD}_i^{exp} - \mathrm{VOD}_i^{calc}}{\mathrm{VOD}_i^{exp}}\right|, \tag{2}$$

$$\mathrm{MaxAE} = \max_{i\in\{1,\ldots,N\}}\left|\frac{\mathrm{VOD}_i^{exp} - \mathrm{VOD}_i^{calc}}{\mathrm{VOD}_i^{exp}}\right|, \tag{3}$$

where N is the total number of explosives considered.

The errors calculated for the explosive dataset considered in this study are summarised in Table 1. The small mean error values (RMSE and MAE) demonstrate the high accuracy of CaThe's predictions, while the MaxAE, being less than 10%, remains well within the acceptable range for

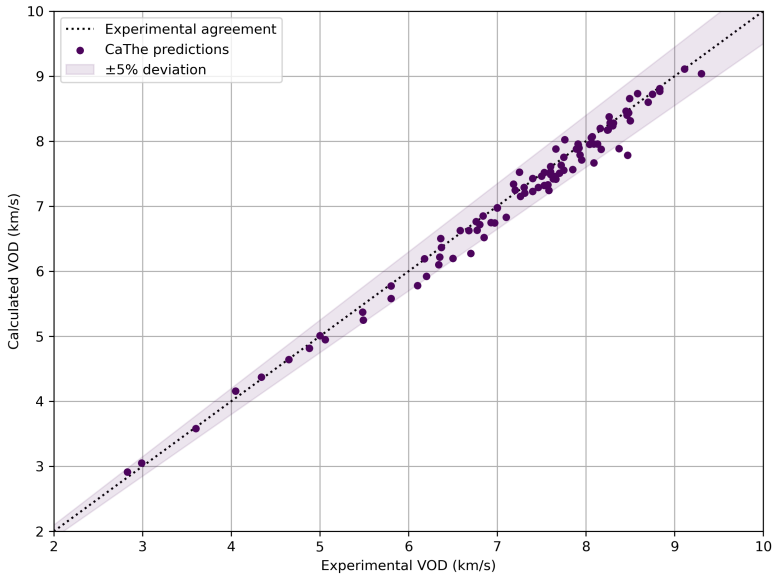

Figure 1: Comparison of calculated against experimental [1] VODs for all explosives considered in this study. Blue scatter points represent CaThe predictions, with the black dotted line indicating perfect agreement. The shaded region shows the range of ±5% deviation from experimental values.

thermochemical software. These results quantitatively highlight CaThe's capability to reliably predict detonation velocities across a wide range of explosives.

Table 1: Summary of errors in VOD predictions obtained by CaThe for the explosives considered in this study, relative to experimental data.

Statistical measure	Value
RMSE	2.5%
MAE	1.87%
MaxAE	8.11%

1.1 VOD vs initial density

To further validate the predictive capabilities of the CaThe thermochemical equilibrium code, we examine the relationship between initial density and detonation velocity for two widely studied explosives: RDX and PETN. Experimental VOD data for each explosive, across a range of initial densities, are compared to CaThe predictions to assess the model's ability to capture density-dependent trends. The details of both explosives are as provided in Table 3 (Appendix A).

Figure 2 illustrates the experimental and predicted detonation velocities for RDX and PETN, as functions of initial density. To account for typical uncertainties associated with detonation velocity measurements, 5% error bars were added to the experimental VODs.

Both sets of data show an expected increase in VOD with increasing density, reflecting the enhanced shock compression and energy release at higher initial densities. The CaThe predictions closely follow the experimental trends for both explosives, underscoring the model's ability to capture these density-dependent effects with high fidelity.

Quantitatively, the deviations between experimental and predicted VODs remain within acceptable limits across the range of densities considered. This strong agreement further demonstrates the robustness and reliability of the CaThe code in modeling the detonation characteristics of high explosives under varying physical conditions.

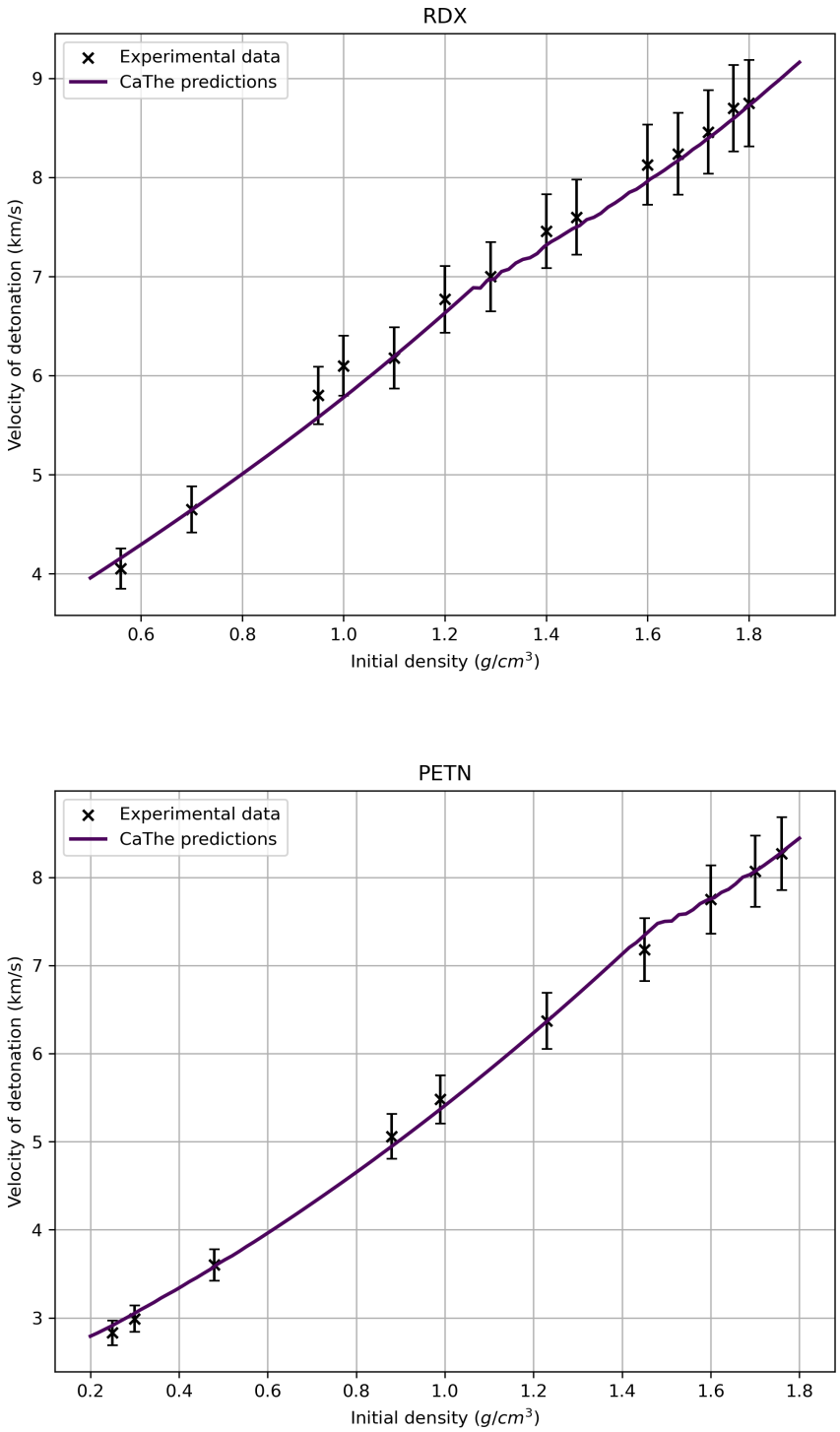

Figure 2: Comparison of experimental [1] and calculated detonation velocities as a function of initial density for RDX (top) and PETN(bottom). The CaThe predictions (solid line) closely follow the experimental data (markers), with 5% error bars shown for the experimental VODs to indicate measurement uncertainties.

2 Isentropic expansion

CaThe is not limited to calculating Chapman-Jouguet (CJ) properties of explosives; it also has the capability to compute their expansion isentrope. Once the CJ point is determined, CaThe calculates points on the expansion isentrope by enforcing a constant entropy condition. To validate this aspect of the module, we calculate the isentropic expansion of five explosives from the database - Composition B, HMX, Nitromethane, PETN and TNT - and compare them with experimentally calibrated reference curves from the literature.

In particular, we compare our calculated isentropes to those presented by Lee et al. [2], where JWL equation of state parameters were calibrated to experimental data obtained from cylinder and sphere tests. JWL is one of the most commonly used equations of state for describing explosive materials in direct numerical simulations, and relies on fitting the following pressure reference curve along the principal isentrope:

$$p_{\text{ref}} = Ae^{-R_1 V/V_0} + Be^{-R_2 V/V_0} + C\left(\frac{V}{V_0}\right)^{-(\omega+1)} \tag{4}$$

The parameters obtained by Lee et al. [2] for the five explosives under consideration are given in Table 2.

Table 2: JWL parameters for the five explosives considered in this study [2]

Explosive	A (Mbar)	B (Mbar)	C (Mbar K^{-1})	R_1	R_2	ω
Comp B	5.24229	0.076783	0.010818	4.2	1.1	0.34
HMX	7.7828	0.07071428	0.006430	4.2	1.0	0.3
Nitromethane	2.0925	0.056895	0.0077042	4.4	1.2	0.3
PETN	7.9653	0.19241	0.006651	4.8	1.2	0.25
TNT	3.71213	0.032306	0.0104527	4.15	0.95	0.30

In Figure 3, we plot the isentrope points calculated by CaThe against the experimentally calibrated JWL reference curves for each explosive. The results show good overall agreement, with minor differences observed between calculation and reference data.

This validation highlights the practical value of CaThe in deriving isentropic data for calibrating equation of state parameters for the detonation products. These calibrated parameters can then be used in direct numerical simulations to study phenomena such as material confinement effects. By enabling the characterisation of a wide range of generic explosive mixtures, CaThe serves as a valuable resource for advancing the study of explosive behaviour.

3 Conclusions

The results summarised in this report demonstrate that CaThe can be confidently used for predicting detonation velocities in both known and novel explosives. The model's ability to handle variations in explosive composition and density, while maintaining high accuracy, is a testament to its robustness and reliability. Additionally, CaThe's capability to model isentropic expansions further highlights its utility in generating equation of state data, which can be used in direct numerical simulations of explosive behavior. This validation not only reinforces the utility of CaThe for explosives design and analysis but also positions it as a powerful tool for applications requiring precise detonation predictions and simulations of complex explosive phenomena.

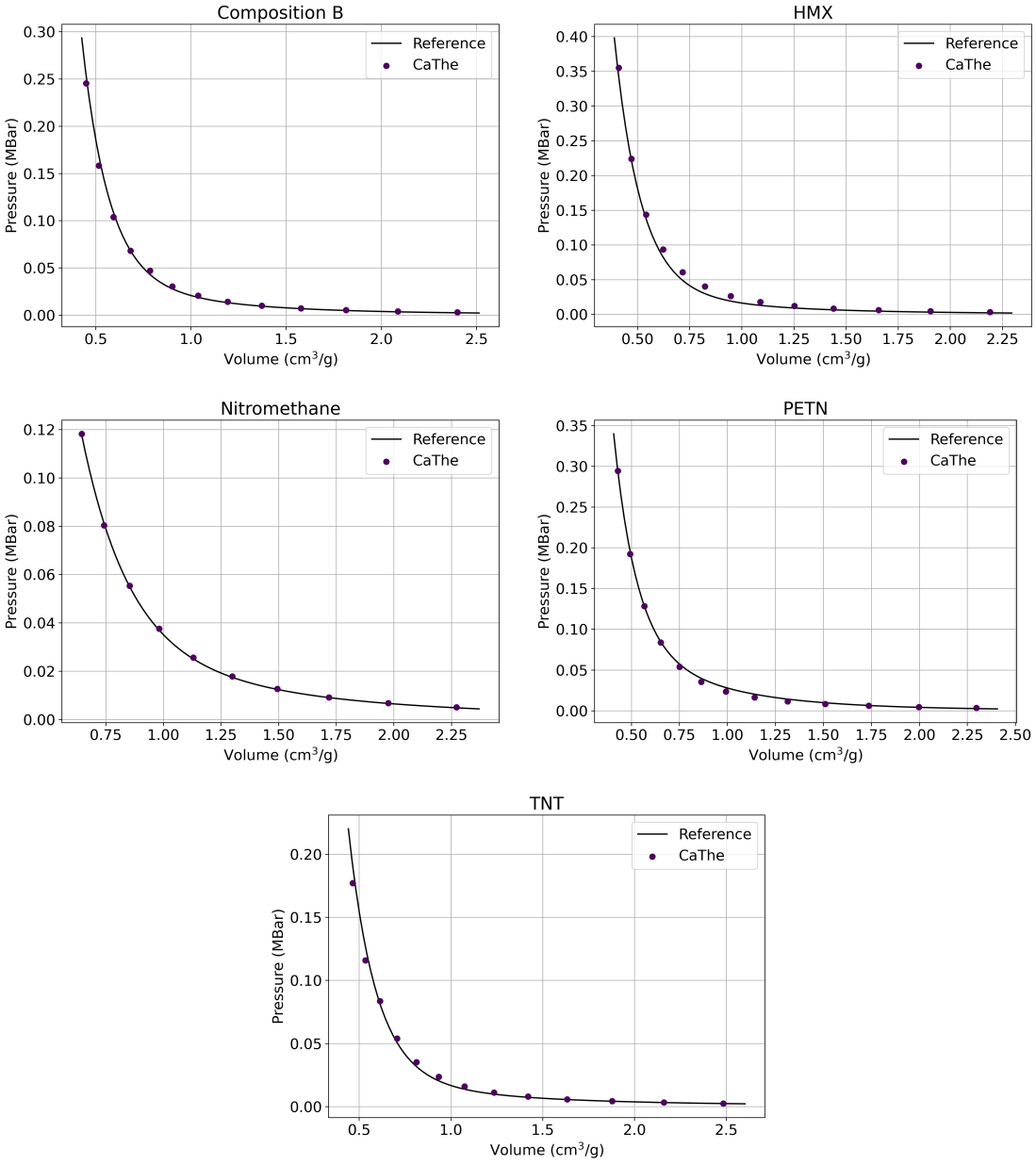

Figure 3: Comparison of isentrope points calculated by CaThe (points) with experimentally calibrated [2] JWL reference curves (solid lines) for five explosives: Composition B, HMX, Nitromethane, PETN, and TNT.

References

[1] Hobbs, M. & Baer, M. Calibrating the BKW-EOS with a large product species data base and measured CJ properties. *Tenth Symposium (International) On Detonation, Boston, MA*. pp. 409-18 (1993)

[2] Lee, E., Hornig, H. & Kury, J. Adiabatic expansion of high explosive detonation products. (Univ. of California Radiation Lab. at Livermore, Livermore, CA (United States),1968)

A Explosive dataset and VOD results

In this section, we present detailed information about the explosives considered in this study. Table 3 includes their initial densities, chemical compositions, heats of formation (HoF), and experimental velocities of detonation. The table also includes the CaThe-predicted velocities of detonation and the corresponding relative error for each explosive, providing a comprehensive overview of the model's accuracy across different explosive types.

Table 3: Properties and CaThe prediction performance for the explosives considered in this study. Experimental detonation velocities are sourced from [1] and "HoF" refers to the heat of formation.

Explosive	Density (kg/m^3)	C (mol)	H (mol)	N (mol)	O (mol)	HoF (kcal/mol)	Exp. VOD (km/s)	CaThe VOD (km/s)	Error (%)
ABH	1.64	24	6	14	24	116	7.2	7.25	0.7
COMP A-3	1.64	1.87	3.74	2.46	2.46	2.84	8.47	7.78	-8.11
COMP B	1.72	2.03	2.64	2.18	2.67	1	7.92	7.9	-0.28
COMP B-3	1.72	2.043	2.501	2.149	2.677	1.332	7.89	7.88	-0.1
COMP C-3	1.6	1.9	2.83	2.34	2.6	-6.45	7.63	7.42	-2.71
COMP C-4	1.66	1.82	3.54	2.46	2.51	3.33	8.37	7.88	-5.81
CYCLOTOL-78/22	1.76	1.731	2.591	2.397	2.688	3.713	8.31	8.28	-0.38
CYCLOTOL-77/23	1.74	1.749	2.586	2.384	2.687	3.58	8.25	8.18	-0.86
CYCLOTOL-75/25	1.76	1.783	2.576	2.356	2.686	3.316	8.3	8.24	-0.75
CYCLOTOL-75/25	1.62	1.783	2.576	2.356	2.686	3.316	7.95	7.71	-2.96
CYCLOTOL-70/30	1.73	1.87	2.551	2.287	2.683	2.654	8.06	8.05	-0.1
CYCLOTOL-65/35	1.72	1.957	2.526	2.218	2.68	1.993	8.04	7.95	-1.11
CYCLOTOL-60/40	1.74	2.043	2.501	2.149	2.677	1.332	8.09	7.96	-1.64
CYCLOTOL-60/40	1.72	2.043	2.501	2.149	2.677	1.332	7.9	7.88	-0.22
CYCLOTOL-50/50	1.63	2.216	2.451	2.011	2.671	0.009	7.66	7.42	-3.2
DATB	1.8	6	5	5	6	-23.6	7.6	7.61	0.15
DATB	1.78	6	5	5	6	-23.6	7.6	7.53	-0.92
DEGN	1.38	4	8	2	7	-99.4	6.76	6.77	0.09
DIPM	1.76	2.642	1.321	1.761	2.642	-1.497	7.4	7.43	0.36
EXP D	1.55	6	6	4	7	-94	6.85	6.52	-4.84
EXP D	1.48	6	6	4	7	-94	6.7	6.28	-6.32
HMX	1.89	4	8	8	8	17.93	9.11	9.11	0.02
HMX	1.6	4	8	8	8	17.93	7.91	7.96	0.59
HMX	1.4	4	8	8	8	17.93	7.3	7.29	-0.17
HMX	1.2	4	8	8	8	17.93	6.58	6.63	0.72
HMX	1	4	8	8	8	17.93	5.8	5.77	-0.47
HMX	0.75	4	8	8	8	17.93	4.88	4.82	-1.27
HNAB	1.6	12	4	8	12	67.9	7.31	7.2	-1.49
HNS	1.6	14	6	6	12	18.7	6.8	6.72	-1.22
HNS	1.7	14	6	6	12	18.7	7.0	6.97	-0.41
LX-01	1.24	1.525	3.727	1.694	3.388	-25.776	6.84	6.85	0.18
LX-14	1.84	1.521	2.917	2.588	2.659	1.51	8.83	8.77	-0.71
MEN-II	1.02	2.06	7.06	1.33	3.1	-74.3	5.49	5.25	-4.43
NG	1.6	3	5	3	9	-88.6	7.7	7.51	-2.46
NM	1.13	1	3	1	2	-27.03	6.35	6.22	-2.07
NONA	1.7	18	5	9	18	27.4	7.4	7.23	-2.35
NQ	1.62	1	4	4	2	-22.1	7.93	7.79	-1.78
NQ	1.55	1	4	4	2	-22.1	7.65	7.45	-2.58
OCTOL-76/23	1.81	1.761	2.583	2.374	2.687	3.054	8.45	8.46	0.15
OCTOL-75/25	1.81	1.783	2.576	2.356	2.686	2.889	8.48	8.44	-0.49
OCTOL-60/40	1.8	2.043	2.501	2.149	2.677	0.991	8.16	8.2	0.44

Table 3: (Cont.) Properties and CaThe prediction performance for the explosives considered in this study. Experimental detonation velocities are sourced from [1] and "HoF" refers to the heat of formation.

Explosive	Density (kg/m^3)	C (mol)	H (mol)	N (mol)	O (mol)	HoF (kcal/mol)	Exp. VOD (km/s)	CaThe VOD (km/s)	Error (%)
PBX-9007	1.64	1.97	3.22	2.43	2.44	7.13	8.09	7.67	-5.22
PBX-9011	1.77	1.73	3.18	2.45	2.61	-4.05	8.5	8.32	-2.17
PBX-9205	1.67	1.83	3.14	2.49	2.51	5.81	8.17	7.88	-3.6
PBX-9501	1.84	1.47	2.86	2.6	2.69	2.3	8.83	8.81	-0.25
PENTOLITE	1.71	2.332	2.366	1.293	3.219	-23.657	7.75	7.56	-2.49
PENTOLITE	1.7	2.332	2.366	1.293	3.219	-23.657	7.53	7.52	-0.16
PENTOLITE	1.68	2.332	2.366	1.293	3.219	-23.657	7.65	7.46	-2.53
PENTOLITE	1.64	2.332	2.366	1.293	3.219	-23.657	7.53	7.32	-2.76
PETN	1.76	5	8	4	12	-128.7	8.27	8.28	0.18
PETN	1.7	5	8	4	12	-128.7	8.07	8.07	-0.02
PETN	1.6	5	8	4	12	-128.7	7.75	7.76	0.07
PETN	1.45	5	8	4	12	-128.7	7.18	7.34	2.25
PETN	1.23	5	8	4	12	-128.7	6.37	6.37	-0.08
PETN	0.99	5	8	4	12	-128.7	5.48	5.37	-2.01
PETN	0.88	5	8	4	12	-128.7	5.06	4.95	-2.23
PETN	0.48	5	8	4	12	-128.7	3.6	3.58	-0.57
PETN	0.3	5	8	4	12	-128.7	2.99	3.05	2.06
PETN	0.25	5	8	4	12	-128.7	2.83	2.91	2.99
PICRATOL	1.63	2.747	2.324	1.479	2.747	-23.029	6.97	6.74	-3.23
PICRIC ACID	1.76	6	3	3	7	-51.3	7.57	7.33	-3.16
PICRIC ACID	1.71	6	3	3	7	-51.3	7.26	7.15	-1.51
PICRIC ACID	1.6	6	3	3	7	-51.3	7.1	6.83	-3.76
RDX	1.8	3	6	6	6	14.71	8.75	8.72	-0.33
RDX	1.77	3	6	6	6	14.71	8.7	8.6	-1.18
RDX	1.72	3	6	6	6	14.71	8.46	8.4	-0.72
RDX	1.66	3	6	6	6	14.71	8.24	8.17	-0.86
RDX	1.6	3	6	6	6	14.71	8.13	7.96	-2.13
RDX	1.46	3	6	6	6	14.71	7.6	7.49	-1.46
RDX	1.4	3	6	6	6	14.71	7.46	7.29	-2.29
RDX	1.29	3	6	6	6	14.71	7.0	6.98	-0.29
RDX	1.2	3	6	6	6	14.71	6.77	6.63	-2.03
RDX	1.1	3	6	6	6	14.71	6.18	6.2	0.24
RDX	1	3	6	6	6	14.71	6.1	5.78	-5.26
RDX	0.95	3	6	6	6	14.71	5.8	5.58	-3.81
RDX	0.7	3	6	6	6	14.71	4.65	4.64	-0.13
RDX	0.56	3	6	6	6	14.71	4.05	4.16	2.64
TACOT	1.85	12	4	8	8	110.5	7.25	7.52	3.77
TATB	1.88	6	6	6	6	-36.85	7.76	8.02	3.4
TATB	1.85	6	6	6	6	-36.85	7.66	7.88	2.87
TETRYL	1.73	7	5	5	8	4.67	7.72	7.63	-1.13
TETRYL	1.71	7	5	5	8	4.67	7.85	7.56	-3.66
TETRYL	1.68	7	5	5	8	4.67	7.5	7.46	-0.49
TETRYL	1.61	7	5	5	8	4.67	7.58	7.24	-4.43
TETRYL	1.36	7	5	5	8	4.67	6.68	6.63	-0.81
TETRYL	1.2	7	5	5	8	4.67	6.34	6.1	-3.79
TNT	1.64	7	5	3	6	-15	6.93	6.75	-2.58
TNT	1.45	7	5	3	6	-15	6.5	6.2	-4.66
TNT	1.36	7	5	3	6	-15	6.2	5.92	-4.51
TNT	1	7	5	3	6	-15	5.0	5.01	0.16
TNT	0.8	7	5	3	6	-15	4.34	4.37	0.77
BTF	1.86	6	0	6	6	144.5	8.49	8.66	1.97
BTF	1.76	6	0	6	6	144.5	8.26	8.38	1.42
HNB	1.97	6	0	6	12	15.7	9.3	9.04	-2.82
TNM	1.64	1	0	4	8	13	6.36	6.5	2.28
TNTAB	1.74	6	0	12	6	270	8.58	8.73	1.76